Concept for Measuring and Compensating Array Deformation

J. J. M de Wit [#1], W. L. van Rossum [#2], M. P. G. Otten [#3], A. G. P. Koekenberg [*4]

[#]*TNO Defence, Security and Safety*
P.O. Box 96864, 2509 JG The Hague, The Netherlands
[1]jacco.dewit@tno.nl
[2]wim.vanrossum@tno.nl
[3]matern.otten@tno.nl

[*]*Dutch Space*
P.O. Box 32070, 2303 DB Leiden, The Netherlands
[4]l.koekenberg@dutchspace.nl

***Abstract*— Phased array antennas are increasingly used in modern radar systems. Such systems are very liable to distortion of the relative phases between the radiating elements. For airborne, spaceborne, and naval phased array systems, vibrations of the array structure are an important source of phase distortions. In this paper, a system concept will be presented to measure array deformation and provide phase compensation information with which the received data can be corrected. Such real-time measurement and compensation of array vibrations may considerably improve the performance of operational systems. Therefore, a study was started to investigate the feasibility of this concept. Shaker experiments proved that the required measurement accuracy is within reach using off-the-shelf sensors and suitable signal processing.**

I. Introduction

In modern radar systems, phased array antennas are often applied. Array antennas consist of many individual radiating elements. For large array antennas, the number of elements may run into the hundreds or even thousands. The radiation pattern of the complete array antenna is determined by the relative phases and amplitudes of the signals applied to the separate elements. By properly adjusting the phases and amplitudes, the antenna beam can be steered. The capability of electronically steering the antenna beam renders slow mechanical joints that are very liable to wear superfluous. Moreover, it offers the possibility to steer the antenna beam from one position to another without inertia. This enables a radar system to track several widespread targets simultaneously, which is a key feature for modern and future radar systems.

Since the radiation pattern of the complete array is controlled by the relative phases between the elements, phase errors are a major concern regarding phased arrays. Distortion of the relative phases may result in severe degradation of the radiation pattern; i.e. widening of the main beam or increase of the sidelobe level. Mismatches within the radar system itself are an important source of phase errors. As a consequence, proper calibration of all electronic components is a prerequisite. However, external sources of phase errors may seriously affect the radiation pattern as well. Examples of external causes of phase errors are vibration of the array structure as a whole and relative motion or vibration of the elements [1]. Vibrations of the array structure are especially a problem when the radar system is mounted on a naval, airborne, or spaceborne platform [2], [3].

Vibration and bending of the array structure may induce significant displacement of the radiating elements relative to each other. Element misalignments of a fraction of the wavelength may already severely degrade the radiation pattern. At radar wavelengths this is just a few millimeters. At TNO a study was initiated to investigate the feasibility to measure array vibrations and provide phase compensation information with which the measured data can be corrected near real-time. To our knowledge, such a real-time measurement and correction of array vibrations has, as yet, never been applied in an operational system.

II. Effects of Array Deformation

The effect of array vibrations does not only depend upon the nature of the motion, e.g. low-frequency or high-frequency, but also on the radar mode of operation. Moving target indication (MTI) and space-time adaptive processing (STAP) modes exploit the phase difference between the receive channels and are therefore very susceptible to array deformation. Synthetic aperture radar (SAR) modes, on the other hand, utilize the sum (Σ) channel. The performance of SAR modes is less affected by array deformation. Therefore, the future detailed study on the effects of array deformation will focus on radar modes exploiting the difference (Δ) channels.

In order to get some insight in allowable mechanical deformation a basic analysis has already been performed. In this analysis a simple two-panel X-band array is considered and the array factor [4] is calculated for different (static) panel misalignments. Only misalignments in the direction of radiation are considered, since these are assumed to be worst-case. The array factor has been calculated for different misalignments, increasing from 10 μm to 200 μm. The results of this analysis are shown in Fig. 1.

Fig. 1(a) shows that the effect on the main lobe and the sidelobes of the Σ pattern is minor. Just the first nulls of the

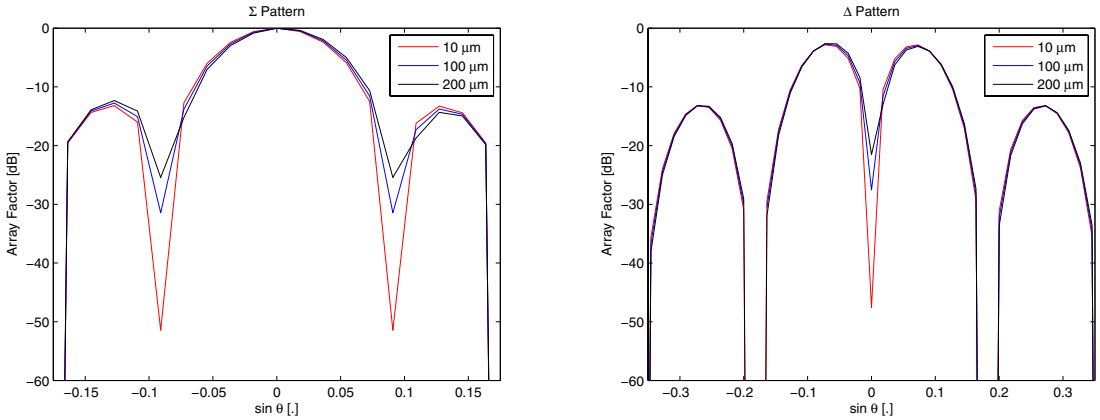

(a) The Σ array factor for different panel misalignments.

(b) The Δ array factor for different panel misalignments.

Fig. 1. The Σ and Δ array factors for different values of the panel misalignment.

Σ pattern are affected. For the Δ pattern, the overall picture is similar; the null at $\sin(\theta) = 0$ is mainly affected. However, for MTI and STAP modes, the relative depth of this null is an important figure of merit, since it is a measure for the clutter mitigation factor.

For many applications, 25 to 30 dB clutter mitigation is sufficient. From Fig. 1(b) it can be seen that in that case the allowable panel misalignment is 100 μm. For a large misalignment, 200 μm in this analysis, only 20 dB clutter mitigation is achieved, which will not suffice for most applications. When the misalignment is negligibly small, i.e. 10 μm in this analysis, the clutter mitigation factor is 45 dB, which is more than adequate.

Thus summarizing, this quick analysis showed that the maximum allowable panel misalignment is of the order of 100 μm (at X-band). Therefore, in order to calculate proper phase corrections, the misalignments must be measured with an accuracy much better than 100 μm.

III. Measurement System Concept

The concept for the measurement system is to attach several accelerometers and an inertial measurement unit (IMU) to the array structure. The accelerometers are used to measure the high-frequency vibrations of the individual elements or array panels, whereas the IMU is used to measure the low-frequency motion of the array structure as a whole. By combining the measurements of all sensors, the attitude and deformations of the structure can be computed. Subsequently, phase corrections can be calculated in order to compensate the effects of array deformation. Whether this is a feasible strategy, regarding e.g. measurement accuracy and signal processing approach, is yet to be determined. In order to get some insight in the overall accuracy to be expected, shaker experiments with off-the-shelf sensors have been carried out. The shaker experiments were performed in close co-operation with Dutch Space.

During the first trials, two different types of sensors were tested; an analog accelerometer and a digital accelerometer providing built-in signal conditioning and analysis. The main advantage of an analog sensor is that it offers full control over for instance sample rate, number of bits, and possible signal filtering. However, in sizeable aircraft and vessels, the distance between the sensors and the data acquisition equipment may be large. In that case, a digital sensor with internal signal conditioning and amplification may be favorable. The trials showed however that the standard off-the-shelf digital sensor was not suitable for highly accurate acceleration measurements. Therefore, it was decided to use analog sensors throughout the shaker experiments.

The shaker experiments were carried out with a metal strip with an end mass of 1 kg attached to a rigid test rig. Vibrations were induced with the aid of an exciter, see Fig. 2. By adapting the length of the strip, the fundamental vibration frequency could be tuned from 10 to 50 Hz, the amplitude could be tuned from 20 to 500 μm. In order to allow the simultaneous excitation of two fundamental frequencies, a second mass was added to the metal strip in a later stage of the experiments. A single-axis Endevco 7201-10-50 piezoelectric accelerometer was attached on top of the end mass. A reference measurement was provided with the aid of a Baumer OADM 12L6460 laser distance sensor, which measured the displacement of the end mass. During the experiments, the acceleration and displacement were measured in vertical direction only.

A. Signal Processing and Kalman Filtering

Obviously, the position of the end mass can be obtained by a double integration of the measured acceleration. However, an integrator acts as a low-pass filter and the calculated position will exhibit a low-frequency drift. This drift can be removed by a linear fit of the position data, but a residual divergence will remain due to the double integration of accelerometer noise.

This is a well-known problem regarding the integration of accelerometer measurements [5]. The effect of accelerometer noise can be reduced by means of redundancy, i.e. the use of several accelerometers. The use of more sophisticated processing, e.g. Kalman filtering, is however mandatory in order to obtain long-term drift-free attitude measurements [6].

In the remainder of this section, the implementation of the Kalman filter will be discussed. The operation of the Kalman filter will be briefly explained in the appendix. For the shaker experiments, the state vector follows as

$$\hat{x}_k = \begin{pmatrix} x_k \\ v_k \\ a_k \end{pmatrix}, \tag{1}$$

in which x is position, v is velocity, and a is acceleration along the z-axis. The initial position, velocity, and acceleration are set to zero. The state transition model is given as

$$F_k = \begin{pmatrix} 1 & \Delta t & \frac{1}{2}\Delta t^2 \\ 0 & 1 & \Delta t \\ 0 & 0 & 1 \end{pmatrix}, \tag{2}$$

where Δt is the time step. The process noise can be calculated as $Q = \Gamma^T \dot{\sigma}_a^2 \Gamma$, in which

$$\Gamma = \begin{pmatrix} \frac{1}{6}\Delta t^3 \\ \frac{1}{2}\Delta t^2 \\ \Delta t \end{pmatrix}, \tag{3}$$

and $\dot{\sigma}_a$ is the expected maximum value of the derivative of the acceleration. The value of $\dot{\sigma}_a$ was derived assuming that the worst-case motion is a 50 Hz sinusoidal with an amplitude of 1 mm. The observation can be described as

$$z_k = \begin{pmatrix} 0 \\ a_k \end{pmatrix}. \tag{4}$$

Considering the description of the observations, only a single boundary condition is implemented: the average position should be zero. Because only two elements of the state vector are used, the observation model follows as

$$H_k = \begin{pmatrix} 1 & 0 & 0 \\ 0 & 0 & 1 \end{pmatrix}. \tag{5}$$

Finally, the covariance matrix for the observations is given as

$$R_k = \begin{pmatrix} \sigma_x^2 & 0 \\ 0 & \sigma_a^2 \end{pmatrix}, \tag{6}$$

where σ_x is the position error and σ_a is the error in the acceleration. The allowable position error was set to 1 mm. The acceleration error σ_a was derived from measurements made with the accelerometer when the metal strip was at rest. The value derived for the Endevco accelerometer is 0.08 ms^{-2}.

B. Experimental Results

During the first experiment, the strip was excited with a random-like vibration made up out of three sinusoids with respective frequencies of 15 Hz, 25 Hz, and 70 Hz. These frequencies were chosen arbitrarily, but they are not harmonically related. The combined amplitude was 200 μm, resulting in ineffective clutter mitigation as discussed in Section II. The settings of the Kalman filter were deliberately chosen loose relative to the vibration parameters. These loose settings allow the Kalman filter to fluctuate compared to the reference measurements. Such fluctuations are mainly due to the integration of accelerometer noise.

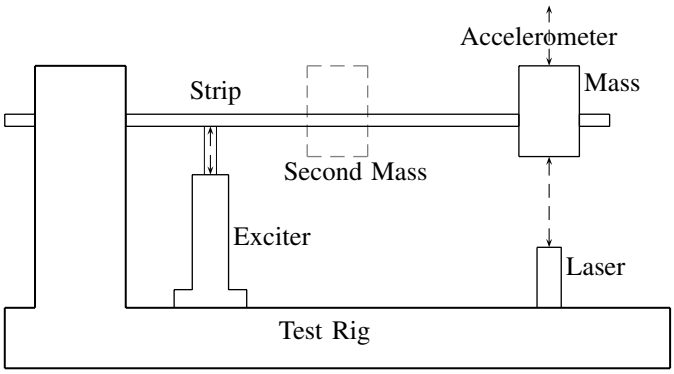

Fig. 2. Diagram of the set-up of the shaker experiments.

As can be seen from Fig. 3(a), the Kalman-filtered data and the reference measurements correspond very well. The measurement accuracy is 13.1 μm, which is well below the desired accuracy of 100 μm. The measurement accuracy is defined as the standard deviation of the measurement error, which is in turn defined as the difference between the Kalman-filtered data and the reference measurement.

The second experiment included an impulse test. The strip was excited with a sinusoidal vibration with a frequency of 9 Hz and an amplitude of 100 μm. After some time an impulse was induced. The results of this experiment are shown in Fig. 3(b). It can be seen that the Kalman-filtered data correspond well to the reference measurement. Mainly in the first oscillation, the Kalman-filter is not capable of tracking the high acceleration values. As a result, the absolute error may be large, up to 350 μm during this experiment, for very short instances. The overall measurement accuracy is nevertheless still below the desired accuracy of 100 μm.

Broadly speaking, SAR mode performance is hardly affected by such an impulse, since the processing interval is relatively long. MTI bursts, on the other hand, are typically very short. Thus a sudden shock may cause several bursts to be lost and MTI mode performance to be degraded to some extent. Whether sudden shocks are likely to occur depends highly on the type of platform.

IV. Conclusion

In modern radar systems phased arrays are increasingly used. Such systems are very sensitive to phase errors. Major external causes of phase errors are relative motion of the elements and vibrations of the array as a whole, in particular for airborne and naval systems. TNO investigated the feasibility to accurately measure array deformations with

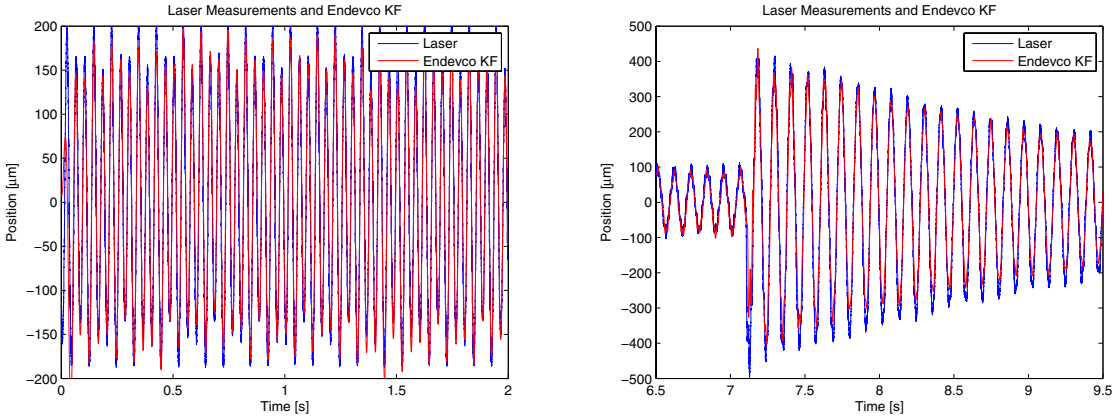

(a) Measurements of a vibration comprising three sinusoids with respective frequencies of 15 Hz, 25 Hz, and 70 Hz and combined amplitude of 200 μm.

(b) Measurements of a 9 Hz sinusoidal vibration with 100 μm amplitude, at 7.1 s an impulse was induced

Fig. 3. Time series of the reference measurements (blue) and the Kalman-filtered Endevco data (red).

accelerometers. The results of some shaker experiments proved that the required accuracy is within reach by using commercial off-the-shelf sensors and proper Kalman-filter processing.

In successive experiments, an IMU will be attached to the test rig and the test rig as a whole will be put in (low-frequency) motion. To some degree, this resembles the situation of an array antenna placed on a moving platform. Consequently, the Kalman filter must be enhanced to integrate different types of measurements of different sensors in different reference frames.

ACKNOWLEDGMENT

The authors wish to thank J. F. M. Lorga, currently employed at Deimos, Lisbon, for his contribution to the project.

REFERENCES

[1] H. S. C. Wang, "Performance of Phased-Array Antennas with Mechanical Errors," *IEEE Trans. Aerosp. Electron. Syst.,* vol. 28, no. 2, pp. 535-545, April 1992.

[2] L. Lightstone, "Antenna Distortions in Multiple Phase Centre Interferometric Systems," in *Proc. IEEE IGARRS,* Pasadena, U.S.A., 1994, pp. 1980-1982.

[3] G. Franceschetti, A. Iodice, S. Maddaluno, and D. Riccio, "Effects of Secondary Antenna Oscillations on X-SAR/SRTM Performance," in *Proc. IEEE IGARSS,* Hamburg, Germany, June 28 - July 2, 1999, pp. 2386-2388.

[4] C. A. Balanis, *Antenna Theory, Analysis and Design,* New York: John Wiley, 1982.

[5] K. Parsa, J. Angeles, and A. K. Misra, "Pose-and-Twist Estimation of a Rigid Body Using Accelerometers," in *Proc. IEEE Int. Conf. Robotics Automation,* Seoul, Korea, May 21-26, 2001, pp. 2873-2878.

[6] H. Rehbinder and X. Hu, "Drift-Free Attitude Estimation for Accelerated Rigid-Bodies,' in *Proc. IEEE Int. Conf. Robotics Automation,* Seoul, Korea, May 21-26, 2001, pp. 4244-4249.

APPENDIX

The Kalman filter comprises two distinct steps; *predict* and *update*. In the predict stage, a prediction of the current state is obtained by using the estimate from the previous time instance. Then, in the update stage, the measurement from the current time instance is used to refine the prediction to arrive at a new, more accurate estimate of the current state. The predicted state vector and covariance matrix follow as

$$\hat{x}_{k|k-1} = F_k \hat{x}_{k-1|k-1} \tag{7}$$

and

$$P_{k|k-1} = F_k P_{k-1|k-1} F_k^T + Q_k \tag{8}$$

respectively. Here, F is the state transition model that describes the dynamics of the system at hand, and Q is the process noise, which is assumed to be Gaussian with zero mean. At time instance k, a measurement or observation of the true state x_k is made according to

$$z_k = H_k x_k + q_k, \tag{9}$$

where H is the observation model, which maps the true state space on to the observed space and q is the observation noise that is assumed to be Gaussian with zero mean and covariance R. The first step in the update stage is done by calculating the innovation and the corresponding covariance

$$y_k = z_k - H_k \hat{x}_{k|k-1} \tag{10}$$

and

$$S_k = H_k P_{k|k-1} H_k^T + R_k, \tag{11}$$

respectively. The optimal Kalman filter gain is given as

$$K_k = P_{k|k-1} H_k^T S_k^{-1}. \tag{12}$$

Consequently, the update is obtained through

$$\hat{x}_{k|k} = \hat{x}_{k|k-1} + K_k y_k \tag{13}$$

and

$$P_{k|k} = (I - K_k H_k) P_{k|k-1}. \tag{14}$$